

University of Groningen

Evidence for cobalt-cobalt bond homolysis and wavelength-dependent CO loss in $(\mu(2)\text{-Alkyne})\text{Co-2(CO)}(6)$ complexes

Boyle, N.M.; Coleman, A.C.; Long, C.; Ronayne, K.L.; Browne, W.R.; Feringa, B.L.; Pryce, M.T.

Published in:
 Inorganic Chemistry

DOI:
[10.1021/ic101321u](https://doi.org/10.1021/ic101321u)

IMPORTANT NOTE: You are advised to consult the publisher's version (publisher's PDF) if you wish to cite from it. Please check the document version below.

Document Version
 Publisher's PDF, also known as Version of record

Publication date:
 2010

[Link to publication in University of Groningen/UMCG research database](#)

Citation for published version (APA):

Boyle, N. M., Coleman, A. C., Long, C., Ronayne, K. L., Browne, W. R., Feringa, B. L., & Pryce, M. T. (2010). Evidence for cobalt-cobalt bond homolysis and wavelength-dependent CO loss in $(\mu(2)\text{-Alkyne})\text{Co-2(CO)}(6)$ complexes. *Inorganic Chemistry*, 49(22), 10214 - 10216.
<https://doi.org/10.1021/ic101321u>

Copyright

Other than for strictly personal use, it is not permitted to download or to forward/distribute the text or part of it without the consent of the author(s) and/or copyright holder(s), unless the work is under an open content license (like Creative Commons).

The publication may also be distributed here under the terms of Article 25fa of the Dutch Copyright Act, indicated by the "Taverne" license. More information can be found on the University of Groningen website: <https://www.rug.nl/library/open-access/self-archiving-pure/taverne-amendment>.

Take-down policy

If you believe that this document breaches copyright please contact us providing details, and we will remove access to the work immediately and investigate your claim.

Downloaded from the University of Groningen/UMCG research database (Pure): <http://www.rug.nl/research/portal>. For technical reasons the number of authors shown on this cover page is limited to 10 maximum.

Supplementary material

Evidence for Cobalt-Cobalt bond homolysis and wavelength dependent CO loss in (μ_2 -alkyne) $\text{Co}_2(\text{CO})_6$ complexes

Nicola M. Boyle, Anthony C. Coleman, Conor Long, Kate L. Ronayne,
Wesley R. Browne, Ben L. Feringa, Mary T. Pryce*

Contents

- 1. General Experimental details S2**
- 2. Synthesis of Metal Carbonyls S3**
- 3. Quantum yield determinations S5**
- 4. Theoretical calculations S15**
- 5. Examples of Time Resolved IR kinetics for Compounds 1 and 2, and IR data for the parent compounds and intermediate produced S21**
- 6. References S23**

1. General Experimental Details

All manipulations were carried out under an atmosphere of argon or nitrogen using standard Schlenk techniques. Silica Gel (Merck) was used as received. All mobile phases for column chromatography were dried over MgSO_4 before use. All solutions were deoxygenated by purging with argon or nitrogen for ~10 min. Column chromatography was carried out using neutral silica gel or neutral aluminum oxide. Diphenyl acetylene, 1-ethynylferrocene, and dicobalt octacarbonyl were obtained from Sigma-Aldrich and used without further purification. Carbon monoxide was obtained from Air Products Ltd. Steady state IR spectra were recorded on a Perkin-Elmer 2000 FTIR spectrophotometer (2 cm^{-1} resolution) in a 0.1 mm sodium chloride liquid cell using spectroscopic grade pentane, cyclohexane, and dichloromethane. NMR spectra were recorded on a Varian VXR-300 (^1H NMR at 300 MHz, ^{13}C NMR at 75.5 MHz), or on a Varian Mercury Plus 400 (^1H NMR at 400 MHz, ^{13}C NMR at 100 MHz). Chemical shifts (δ) are denoted in ppm and referenced to the residual solvent peak unless stated otherwise (CDCl_3 , ^1H $\delta = 7.24$, ^{13}C $\delta = 77.0$). The splitting patterns are designated as follows: s (singlet), d (doublet), dd (double doublet), t (triplet), q (quartet), m (multiplet), and br (broad). Coupling constants (J) between two nuclei separated by n chemical bonds are denoted in hertz (Hz). Chemical ionisation mass spectra (MS-CI+), electron impact (MS-EI+), and exact mass determination (HRMS) were recorded on a AEI MS-902 or Applied Biosystems Q-STAR mass spectrometer. Electrospray ionisation mass spectrometry (MS-ESI+) was performed on a Triple Quadrupole LC-MS-MS mass spectrometer (API 3000, Perkin-Elmer Sciex Instruments). UV-vis spectra were recorded on a Hewlett-Packard 8453 diode array. Picosecond time resolved infra-red spectroscopy were carried out as described previously.ⁱ

2. Synthesis

2-(Phenylethynyl)thiophene was prepared via the Sonogashira coupling reaction.ⁱⁱ Anhydrous triethylamine was added to a round bottom flask, purged with argon for 10 min and then charged with 2-bromothiophene (3.0 mmol, 0.29 ml). Following this a catalytic quantity of bis(triphenylphosphine)palladium(II)chloride (0.06 mmol, 42 mg, 2 %), triphenylphosphine (0.12 mmol, 32 mg, 4%) and cuprous iodide (0.06 mmol, 11 mg, 2 %) were added to the flask followed by 1-phenylacetylene (4.5 mmol, 0.63 ml) in rapid succession. The reaction mixture was heated under a gentle reflux overnight under an inert atmosphere and then allowed to cool to room temperature. Solvent and excess aryl alkyne were removed in vacuo. The crude product was extracted from the brown oil by first washing in *ca.* 5 ml of dichloromethane followed by the addition of *ca.* 25 ml of hexane. The solvent was then decanted off. This process was repeated several times until the washings remained colourless. The washings were combined and dried over magnesium sulphate. The solvent was then removed in vacuo affording a viscous oil. The crude product was purified by Kugelrohr distillation (160 °C, 0.04 mmHg) affording a white solid. Yield: 502 mg, 2.73 mmol, 91 %. Spectroscopic data were in agreement with reported data.ⁱⁱⁱ ¹H-NMR (CDCl₃): δ 7.54 – 7.51 (2H, m), 7.37 – 7.34 (3H, m), 7.30 – 7.29 (2H, m), 7.01 (1H, dd, *J* = 4.8, 3.9 Hz). ¹³C-NMR (CDCl₃): δ 131.93, 131.44, 128.45, 128.40, 127.29, 127.13, 123.34, 122.94. IR (pentane) ν (C≡C): 2130cm⁻¹, m.p. = 51-52 °C.

(μ₂-C₆H₅CCC₆H₅)Co₂(CO)₆ (1)

(μ₂-C₆H₅CCC₆H₅)Co₂(CO)₆ (1) was prepared according to the method outlined by Champeil and Draper^{iv} with minor modifications. Diphenylacetylene (1.12 mmol / 200 mg) was dissolved in 30 ml of hexane and purged with nitrogen for 10 min. Dicobalt octacarbonyl (1.12 mmol / 384 mg) was added to the reaction vessel and stirred under a stream of nitrogen for 20 h (in the dark). The product mixture (deep red) was purified by column chromatography on silica using petroleum ether (40:60) as mobile phase. A deep red fraction was collected and the solvent removed in vacuo. Yield: 483 mg, 1.04 mmol, 93 %. ¹H-NMR (400 MHz, CDCl₃): δ 7.60 (2H, m), 7.58 (2H, m), 7.39-7.37 (3H, m), 7.35-7.33 (3H, m), IR (*n*-pentane): ν (CO) 2026, 2055, 2089 cm⁻¹.

(μ_2 -C₆H₅CCC₄H₄S)Co₂(CO)₆ (2**)**

(μ_2 -C₆H₅CCC₄H₄S)Co₂(CO)₆ (**2**) was prepared in a manner similar to that described above. 2-phenylethynyl-thiophene (0.80 mmol / 150 mg) was dissolved in 30 ml of hexane and purged with nitrogen for 10 min. Dicobalt octacarbonyl (0.85 mmol / 290 mg) was then added to the reaction vessel and stirred under a stream of nitrogen for 20 h (in the dark). The product mixture (deep red) was purified by column chromatography on silica using petroleum ether (40:60) as mobile phase. A deep red fraction was collected and the solvent removed in vacuo. Yield: 338 mg, 0.72 mmol, 90 %.

¹H-NMR (600 MHz, CDCl₃): δ 7.70-7.68 (2H, m), 7.42-7.35 (5H, m), 7.06-7.04 (1H, m); ¹³C-NMR (CDCl₃), δ 198.6, 141.6, 137.2, 137.6, 128.9, 128.7, 128.4, 127.9, 126.7, 91.6, 82.0. IR (*n*-pentane): ν (CO) 2034, 2062, 2095 cm⁻¹.

(μ_2 -Ethynylferrocene)Co₂(CO)₆ (3**)**

(μ_2 -Ethynylferrocene)Co₂(CO)₆ (**3**) was prepared in a similar manner. Ethynylferrocene (0.95 mmol / 200 mg) was dissolved in 30 ml of hexane and purged with nitrogen for 10 min. Dicobalt octacarbonyl (0.93 mmol / 320 mg) was added to the reaction vessel and stirred under a stream of nitrogen for 18 h (in the dark). The product mixture (deep green) was purified by column chromatography on silica using petroleum ether (40:60) as mobile phase. A deep green fraction was collected and the solvent removed in vacuo. Yield: 210 mg, 0.42 mmol, 44 %. Spectroscopic data were in good agreement with reported data.

¹H NMR (400 MHz, CDCl₃): 6.28 (s, 1H) , 4.38 (d, 2H), 4.32 (s, 5H), 4.16 (d, 2H); ¹³C-NMR (100 MHz, CDCl₃): δ 75-76 (C \equiv C), 69.2 (α , Cp), 70.1 (Cp), 70.5 (β , Cp); IR (CH₂Cl₂): ν (CO) 2091, 2053, 2030, 2024 and 2210 cm⁻¹; Mass Spec.: E.I m/z 328 (-6 x CO), 356 (-5 x CO); HRMS (E.I.) calcd. for C₁₈ H₁₀O₆Co₂Fe: 495.8491, found 495.8514; Anal. Calcd. for C₁₈ H₁₀O₆Co₂Fe: C 43.59 %, H 2.03 %, Found C 43.46 %, 1.99 %

3. Quantum yield determinations

Photochemical quantum yields were determined by actinometry using potassium ferrioxalate as the reference reaction.^v Solutions of complexes **1-3** were irradiated at each excitation wavelength in pentane, with PPh₃ (10% molar excess) as trapping agent, Irradiation was achieved using band pass filtering of the output of a 150 W Hg arc lamp. Conversions of the starting materials were driven to a maximum of 10%, to minimize the effect of product absorption at the excitation wavelength. Changes in absorbance were monitored at 400 nm, which corresponds to λ_{max} of the photoproduct, as displayed in figure 1.

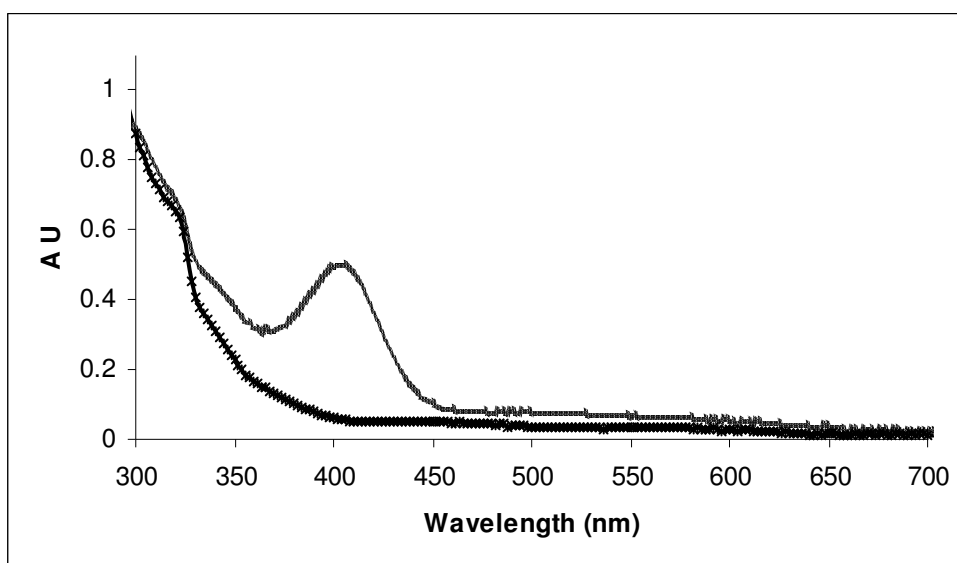


Figure 1. UV-vis spectra for $(\mu_2\text{-C}_6\text{H}_5\text{CCC}_4\text{H}_4\text{S})\text{Co}_2(\text{CO})_6$ (**2**) (solid dark line) and $(\mu_2\text{-C}_6\text{H}_5\text{CCC}_4\text{H}_4\text{S})\text{Co}_2(\text{CO})_5(\text{PPh}_3)$ (dashed line) in pentane.

Irradiation wavelength				
compound	313 nm	365 nm	405 nm	546 nm
1	0.078	0.035	0.027	0.045
2	0.145	0.080	0.045	0.106
3	0.269	0.071	0.047	0.233

Table 1 Quantum yields for CO-loss for the $(\mu_2\text{-alkyne})\text{Co}_2(\text{CO})_6$ complexes studied.

(a) Quantum yield determinations of CO loss for $[(\mu_2\text{-C}_6\text{H}_5\text{CCC}_6\text{H}_5)\text{Co}_2(\text{CO})_6]$ (1)

Molar excitation coefficients at 400 nm

$(\mu_2\text{-C}_6\text{H}_5\text{CCC}_6\text{H}_5)\text{Co}_2(\text{CO})_6$ (1) $1,140 \text{ L mol}^{-1} \text{ cm}^{-1}$

$(\mu_2\text{-C}_6\text{H}_5\text{CCC}_6\text{H}_5)\text{Co}_2(\text{CO})_5(\text{PPh}_3)$ $8,179 \text{ L mol}^{-1} \text{ cm}^{-1}$

Irradiation of 1 at 313 nm (21 mins)

Increase in intensity of band at 400 nm = 0.16

Molar increase = 2.34×10^{-5} molar

Moles converted per second = 1.9×10^{-8} moles/s

For a 3 cm^3 sample, number of molecules photolysed per second = 3.35×10^{13} molecules/s

Change in absorbance of actinometer solution at 510 nm

Absorbance at 510 nm = 0.8228

Number of Fe^{2+} ions = 6.70×10^{17} ions

Using a quantum yield for Fe^{2+} production of 1.24 at 313 nm

Number of photons emitted by the source at 313 nm = 5.40×10^{17}

Number of photons emitted per second by the source at 313 nm = 4.29×10^{14} photons/s

Number of photons absorbed by the sample = 4.29×10^{14} photons/s

Quantum yield of photochemical reaction is $(3.35 \times 10^{13}) / (4.29 \times 10^{14}) = 0.078$

Irradiation of 1 at 365 nm (20 mins)

Increase in intensity of band at 400 nm = 0.15

Molar increase = 2.19×10^{-5} molar

Moles converted per second = 1.8×10^{-8} moles/s

For a 3 cm^3 sample, number of molecules photolysed per second = 3.30×10^{13} molecules/s

Change in absorbance of actinometer solution at 510 nm

Absorbance at 510 nm = 1.70

Number of Fe^{2+} ions = 1.39×10^{18} ions

Using a quantum yield for Fe^{2+} production of 1.21 at 365 nm

Number of photons emitted by the source at 365 nm = 5.40×10^{17}

Number of photons emitted per second by the source at 313 nm = 9.56×10^{14} photons/s

Number of photons absorbed by the sample = 9.56×10^{14} photons/s

Quantum yield of photochemical reaction is $(3.30 \times 10^{13}) / (9.56 \times 10^{14}) = 0.035$

Irradiation of 1 at 405 nm (15 mins)

Increase in intensity of band at 400 nm = 0.074

Molar increase = 1.09×10^{-5} molar

Moles converted per second = 1.2×10^{-8} moles/s

For a 3 cm^3 sample, number of molecules photolysed per second = 2.19×10^{13} molecules/s

Change in absorbance of actinometer solution at 510 nm

Absorbance at 510 nm = 1.02

Number of Fe^{2+} ions = 8.31×10^{17} ions

Using a quantum yield for Fe^{2+} production of 1.14 at 405 nm

Number of photons emitted by the source at 405 nm = 7.29×10^{17}

Number of photons emitted per second by the source at 405 nm = 8.10×10^{14} photons/s

Number of photons absorbed by the sample = 8.10×10^{14} photons/s

Quantum yield of photochemical reaction is $(2.19 \times 10^{13}) / (8.10 \times 10^{14}) = 0.027$

Irradiation of 1 at 546 nm (60 mins)

Increase in intensity of band at 400 nm = 0.114

Molar increase = 1.69×10^{-5} molar

Moles converted per second = 5.0×10^{-9} moles/s

For a 3 cm^3 sample, number of molecules photolysed per second = 8.47×10^{12} molecules/s

Change in absorbance of actinometer solution at 510 nm

Absorbance at 510 nm = 0.123

Number of Fe^{2+} ions = 1.00×10^{17} ions

Using a quantum yield for Fe^{2+} production of 0.15 at 546 nm

Number of photons emitted by the source at 546 nm = 6.68×10^{17}

Number of photons emitted per second by the source at 546 nm = 1.87×10^{14} photons/s

Number of photons absorbed by the sample = 1.87×10^{14} photons/s

Quantum yield of photochemical reaction is $(8.47 \times 10^{12}) / (1.87 \times 10^{14}) = 0.045$

(b) Quantum yield determinations of $[(\mu_2\text{-C}_6\text{H}_5\text{CCC}_4\text{H}_4\text{S})\text{Co}_2(\text{CO})_6]$ (2**)**

Molar excitation coefficients at 400 nm

$(\mu_2\text{-C}_6\text{H}_5\text{CCC}_4\text{H}_4\text{S})\text{Co}_2(\text{CO})_6$ (**2**) $2,314 \text{ L mol}^{-1} \text{ cm}^{-1}$

$(\mu_2\text{-C}_6\text{H}_5\text{CCC}_4\text{H}_4\text{S})\text{Co}_2(\text{CO})_5(\text{PPh}_3)$ $4,829 \text{ L mol}^{-1} \text{ cm}^{-1}$

Irradiation of 2 at 313 nm (10 mins)

Increase in intensity of band at 400 nm = 0.077

Molar increase = 3.07×10^{-5} molar

Moles converted per second = 5.1×10^{-8} moles/s

For a 3 cm^3 sample, number of molecules photolysed per second = 9.21×10^{13} molecules/s

Change in absorbance of actinometer solution at 510 nm

Absorbance at 510 nm = 0.5862

Number of Fe^{2+} ions = 4.77×10^{17} ions

Using a quantum yield for Fe^{2+} production of 1.24 at 313 nm

Number of photons emitted by the source at 313 nm = 3.85×10^{17}

Number of photons emitted per second by the source at 313 nm = 6.41×10^{14} photons/s

Number of photons absorbed by the sample = 6.41×10^{14} photons/s

Quantum yield of photochemical reaction is $(9.21 \times 10^{13}) / (6.41 \times 10^{14}) = 0.145$

Irradiation of 2 at 365 nm (15 min)

Increase in intensity of band at 400 nm = 0.099

Molar increase = 3.94×10^{-5} molar

Moles converted per second = 4.4×10^{-8} moles/s

For a 3 cm^3 sample, number of molecules photolysed per second = 7.91×10^{13} molecules/s

Change in absorbance of actinometer solution at 510 nm

Absorbance at 510 nm = 1.3191

Number of Fe^{2+} ions = 1.07×10^{18} ions

Using a quantum yield for Fe^{2+} production of 1.21 at 365 nm

Number of photons emitted by the source at 365 nm = 8.87×10^{17}

Number of photons emitted per second by the source at 313 nm = 9.85×10^{14} photons/s

Number of photons absorbed by the sample = 9.85×10^{14} photons/s

Quantum yield of photochemical reaction is $(7.91 \times 10^{13}) / (9.85 \times 10^{14}) = 0.080$

Irradiation of 2 at 405 nm (15 mins)

Increase in intensity of band at 400 nm = 0.046

Molar increase = 1.83×10^{-5} molar

Moles converted per second = 2.0×10^{-8} moles/s

For a 3 cm^3 sample, number of molecules photolysed per second = 3.67×10^{13} molecules/s

Change in absorbance of actinometer solution at 510 nm

Absorbance at 510 nm = 1.02

Number of Fe^{2+} ions = 8.31×10^{17} ions

Using a quantum yield for Fe^{2+} production of 1.14 at 405 nm

Number of photons emitted by the source at 405 nm = 7.29×10^{17}

Number of photons emitted per second by the source at 405 nm = 8.10×10^{14} photons/s

Number of photons absorbed by the sample = 8.10×10^{14} photons/s

Quantum yield of photochemical reaction is $(3.67 \times 10^{13}) / (8.10 \times 10^{14}) = 0.045$

Irradiation of 2 at 546 nm (40 mins)

Increase in intensity of band at 400 nm = 0.073

Molar increase = 2.91×10^{-5} molar

Moles converted per second = 1.2×10^{-9} moles/s

For a 3 cm^3 sample, number of molecules photolysed per second = 2.19×10^{13} molecules/s

Change in absorbance of actinometer solution at 510 nm

Absorbance at 510 nm = 0.0907

Number of Fe^{2+} ions = 7.38×10^{16} ions

Using a quantum yield for Fe^{2+} production of 0.15 at 546 nm

Number of photons emitted by the source at 546 nm = 4.92×10^{17}

Number of photons emitted per second by the source at 546 nm = 2.05×10^{14} photons/s

Number of photons absorbed by the sample = 2.05×10^{14} photons/s

Quantum yield of photochemical reaction is $(2.19 \times 10^{13}) / (2.05 \times 10^{14}) = 0.106$

(c) Quantum yield determinations of $[(\mu_2\text{-Ethynylferrocene})\text{Co}_2(\text{CO})_6]$ (3**)**

Molar excitation coefficients at 400 nm

$(\mu_2\text{-Ethynylferrocene})\text{Co}_2(\text{CO})_6$ (**3**) $1,497 \text{ L mol}^{-1} \text{ cm}^{-1}$

$(\mu_2\text{-Ethynylferrocene})\text{Co}_2(\text{CO})_5(\text{PPh}_3)$ $2,717 \text{ L mol}^{-1} \text{ cm}^{-1}$

Irradiation of 3 at 313 nm (20mins)

Increase in intensity of band at 400 nm = 0.072

Molar increase = 1.21×10^{-4} molar

Moles converted per second = 1.0×10^{-7} moles/s

For a 3 cm^3 sample, number of molecules photolysed per second = 1.81×10^{14} molecules/s

Change in absorbance of actinometer solution at 510 nm

Absorbance at 510 nm = 1.2258

Number of Fe^{2+} ions = 9.98×10^{17} ions

Using a quantum yield for Fe^{2+} production of 1.24 at 313 nm

Number of photons emitted by the source at 313 nm = 8.04×10^{17}

Number of photons emitted per second by the source at 313 nm = 6.71×10^{14} photons/s

Number of photons absorbed by the sample = 6.71×10^{14} photons/s

Quantum yield of photochemical reaction is $(1.81 \times 10^{14}) / (6.71 \times 10^{14}) = 0.269$

Irradiation of 3 at 365 nm (25 mins)

Increase in intensity of band at 400 nm = 0.084

Molar increase = 6.68×10^{-5} molar

Moles converted per second = 4.6×10^{-8} moles/s

For a 3 cm^3 sample, number of molecules photolysed per second = 8.26×10^{13} molecules/s

Change in absorbance of actinometer solution at 510 nm

Absorbance at 510 nm = 1.993

Number of Fe^{2+} ions = 1.62×10^{18} ions

Using a quantum yield for Fe^{2+} production of 1.21 at 365 nm

Number of photons emitted by the source at 365 nm = 1.34×10^{18}

Number of photons emitted per second by the source at 365 nm = 1.16×10^{15} photons/s

Number of photons absorbed by the sample = 1.16×10^{15} photons/s

Quantum yield of photochemical reaction is $(8.26 \times 10^{13}) / (1.16 \times 10^{15}) = 0.071$

Irradiation of 3 at 405 nm (25 mins)

Increase in intensity of band at 400 nm = 0.044

Molar increase = 3.61×10^{-5} molar

Moles converted per second = 2.4×10^{-8} moles/s

For a 3 cm^3 sample, number of molecules photolysed per second = 4.35×10^{13} molecules/s

Change in absorbance of actinometer solution at 510 nm

Absorbance at 510 nm = 1.952

Number of Fe^{2+} ions = 1.59×10^{18} ions

Using a quantum yield for Fe^{2+} production of 1.14 at 405 nm

Number of photons emitted by the source at 405 nm = 1.39×10^{18}

Number of photons emitted per second by the source at 405 nm = 9.30×10^{14} photons/s

Number of photons absorbed by the sample = 9.30×10^{14} photons/s

Quantum yield of photochemical reaction is $(4.35 \times 10^{13}) / (9.30 \times 10^{14}) = 0.047$

Irradiation of 3 at 546 nm (35 mins)

Increase in intensity of band at 400 nm = 0.133

Molar increase = 5.27×10^{-5} molar

Moles converted per second = 2.5×10^{-8} moles/s

For a 3 cm³ sample, number of molecules photolysed per second = 4.54×10^{13} molecules/s

Change in absorbance of actinometer solution at 510 nm

Absorbance at 510 nm = 0.075

Number of Fe²⁺ ions = 6.14×10^{16} ions

Using a quantum yield for Fe²⁺ production of 0.15 at 546 nm

Number of photons emitted by the source at 546 nm = 4.09×10^{17}

Number of photons emitted per second by the source at 546nm = 1.95×10^{14} photons/s

Number of photons absorbed by the sample = 4.09×10^{14} photons/s

Quantum yield of photochemical reaction is $(4.54 \times 10^{13}) / (1.95 \times 10^{14}) = 0.233$

4. Theoretical methods

Initial coordinates for the structural optimization of $(\mu\text{-C}_2\text{H}_2)\text{Co}_2(\text{CO})_6$ were obtained from Platts et al.^{vi} The B3LYP/LANL2DZp model chemistry was used for all the calculations as implemented in Gaussian03.^{vii}

The Hessian matrix was calculated to predict the infrared spectrum of $(\mu\text{-C}_2\text{H}_2)\text{Co}_2(\text{CO})_6$.

The predicted ν_{CO} bands of this complex were corrected by comparison with the published IR spectrum.^{viii} This yielded a correction factor of 1.0222 which was then used to correct the calculated ν_{CO} bands of the equivalent ground state triplet species.

	$\nu_{\text{CO}} \text{ (cm}^{-1}\text{)}$				
Obs.	2097.8	2058.5	2033.7	2028.1	2016.6
Singlet	2097.9	2051.3	2037.6	2035.1	2012.7
Triplet	2087.5	2057.9	2024.1	2021.7	2015.2
$\Delta\nu$	10.3	0.6	9.6	6.3	1.4

Table 1. Observed spectrum and calculated singlet and triplet state spectra for $(\mu\text{-C}_2\text{H}_2)\text{Co}_2(\text{CO})_6$

Mulliken atomic spin densities:

1	Co	1.092758
2	Co	1.092758
3	C	-0.052279
4	C	-0.052279
5	H	-0.009581
6	H	-0.009581
7	C	-0.007863
8	O	-0.017921
9	C	-0.007863
10	O	-0.017921
11	C	-0.007863
12	O	-0.017921
13	C	-0.007863
14	O	-0.017921
15	C	0.044255
16	O	-0.023586
17	C	0.044255
18	O	-0.023586

Sum of Mulliken spin densities= 2.00000

Table 2. Mulliken atomic spin densities: for $^3(\mu\text{-C}_2\text{H}_2)\text{Co}_2(\text{CO})_6$ at UB3LYP/LANL2DZp

TD DFT Results for Singlet to Singlet transitions in $(\mu\text{-C}_2\text{H}_2)\text{Co}_2(\text{CO})_6$

Excitation energies and oscillator strengths:

Excited State 1: Singlet-B1 2.1748 eV 570.09 nm f=0.0013

59 -> 67 -0.12921

66 -> 67 0.64946

This state for optimization and/or second-order correction.

Copying the excited state density for this state as the 1-particle RhoCI density.

Excited State 2: Singlet-B2 2.9485 eV 420.50 nm f=0.0006

57 -> 67 -0.10783

64 -> 67 0.66633

65 -> 67 0.10100

Excited State 3: Singlet-A2 3.0145 eV 411.29 nm f=0.0000

58 -> 67 0.10349

62 -> 67 0.66856

Excited State 4: Singlet-A1 3.0321 eV 408.90 nm f=0.0002

60 -> 67 0.52324

63 -> 67 0.41758

Excited State 5: Singlet-A1 3.0944 eV 400.67 nm f=0.0012

60 -> 67 -0.44065

63 -> 67 0.50257

Excited State 6: Singlet-B2 3.2176 eV 385.33 nm f=0.1090

59 -> 68 -0.10106

61 -> 67 -0.22033

64 -> 67 -0.10484

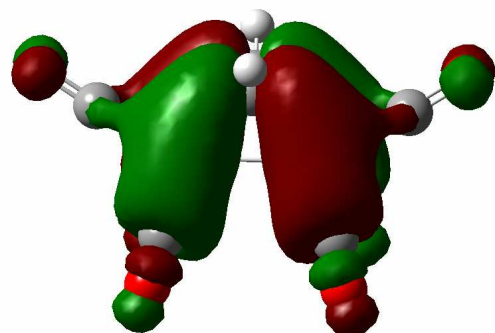
65 -> 67 0.53699

66 -> 72 0.11054

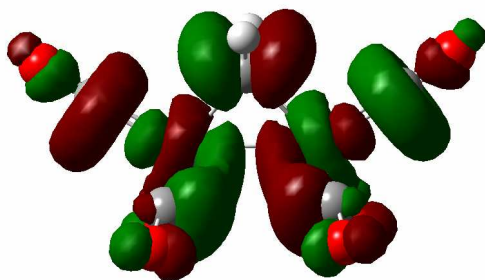
66 -> 76 -0.23921

66 -> 78 0.16302

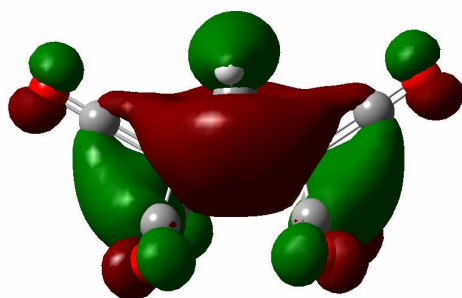
MO 66 HOMO



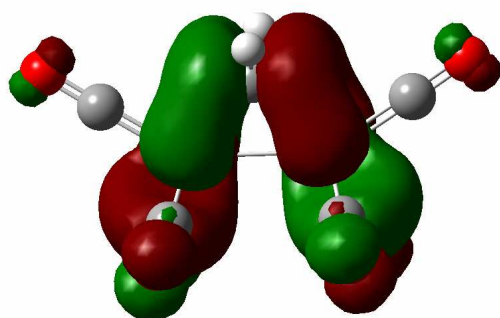
MO67 LUMO



MO64 HOMO-2



MO63 HOMO-3



Energy calculations on parallel and perpendicular structures as per Hoffmann et al. (reference 13 in manuscript)

Repeated attempts to locate a parallel isomer on the singlet potential energy surface using both B3LYP/Lanl2dzp and B3LYP/Tzvp model chemistries failed. However the semi-empirical approach used by Hoffmann (reference 13 in manuscript) was used to estimate the energy of this species and this was compared to the energy of the optimized perpendicular structure at the B3LYP/Tzvp level. The results are outlined in the following table

Based on semi empirical Calculations as per Hoffmann				delta E		
	a.u.	Joules	kJmol-1	kJmol-1	eV	nm
Parallel	-3523.192744	-1.5360233E-14	-9251468.47	490.12	5.079755	244.1062
Perpendicular	-3523.379393	-1.5361047E-14	-9251958.59			

Coordinates used in calculation of energy

Perpendicular

Center Number	Atomic Number	Atomic Type	Coordinates (Angstroms)		
			X	Y	Z
1	27	0	0.000000	1.245131	0.135724
2	27	0	0.000000	-1.245131	0.135724
3	6	0	0.664790	0.000000	1.509350
4	6	0	-0.664790	0.000000	1.509350
5	1	0	1.519242	0.000000	2.164530
6	1	0	-1.519242	0.000000	2.164530
7	6	0	-1.466459	1.550542	-0.909410
8	8	0	-2.392424	1.753069	-1.541215
9	6	0	1.466459	-1.550542	-0.909410
10	8	0	2.392424	-1.753069	-1.541215
11	6	0	-1.466459	-1.550542	-0.909410
12	8	0	-2.392424	-1.753069	-1.541215
13	6	0	1.466459	1.550542	-0.909410
14	8	0	2.392424	1.753069	-1.541215
15	6	0	0.000000	-2.749518	1.110337
16	8	0	0.000000	-3.690341	1.753145
17	6	0	0.000000	2.749518	1.110337
18	8	0	0.000000	3.690341	1.753145

Parallel (using semi empirical approach cf Hoffmann reference 13 in Manuscript)

Center Number	Atomic Number	Atomic Type	Coordinates (Angstroms)		
			X	Y	Z
1	27	0	-1.487486	-0.000006	-0.492449
2	27	0	1.264463	0.000003	0.177477
3	6	0	-0.097841	-0.000007	-1.908892
4	6	0	1.225453	0.000014	-1.778237
5	1	0	-0.667274	-0.000023	-2.852391
6	1	0	2.002389	0.000025	-2.538454
7	6	0	-2.913345	-0.000002	0.600978
8	8	0	-3.852387	0.000001	1.300668
9	6	0	2.068659	-1.590428	0.087772
10	8	0	2.740401	-2.552648	0.003461
11	6	0	0.803169	-0.000010	1.914838
12	8	0	0.483037	-0.000017	3.044055
13	6	0	-1.218637	-1.775736	-0.511149
14	8	0	-1.031831	-2.929402	-0.550616
15	6	0	2.068627	1.590449	0.087789
16	8	0	2.740351	2.552683	0.003490
17	6	0	-1.218640	1.775725	-0.511155
18	8	0	-1.031841	2.929392	-0.550628

5. Examples of Time Resolved IR kinetics for Compounds 1 and 2, and IR data for the parent compounds and intermediate produced

Compound 1			
	CH ₃ CN cm ⁻¹	THF cm ⁻¹	Pentane cm ⁻¹
Parent bands	2092, 2056, 2028	2084, 2050, 2022	2089, 2055, 2031
‘Hot’ species	2072, 2044, 2009	2064, 2036, 2008	2074, 2040, 2016
Triplet diradical	2082, 2048, 2019	2073, 2040, 2012	2079, 2045, 2021

Table 3. IR data for compound **1**, and the bands observed in the IR spectrum following excitation at 400 nm.

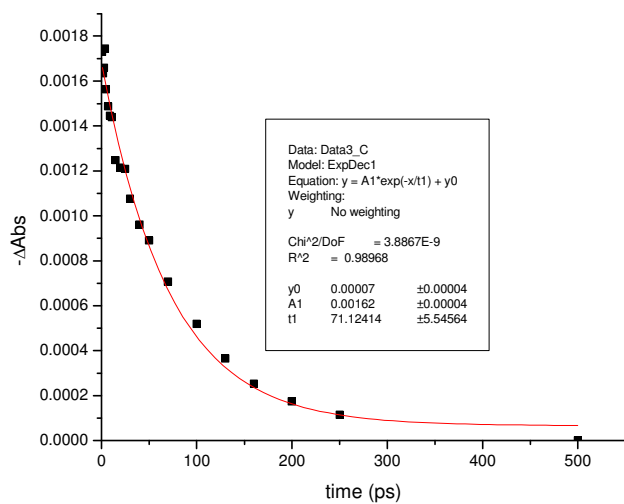
Compound 2			
	CH ₃ CN cm ⁻¹	THF cm ⁻¹	Pentane cm ⁻¹
Parent bands	2093, 2058, 2029	-	-
‘Hot’ species	2078, 2049, 2008	-	-
Triplet diradical	2083, 2052, 2018	-	-

Table 4. IR data for compound **2**, and the bands observed in the IR spectrum following excitation at 400 nm.

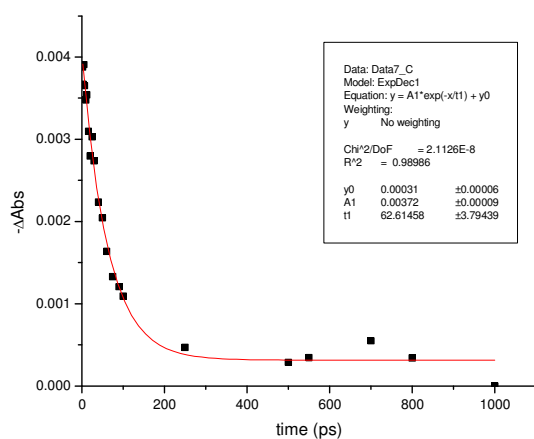
Compound 3			
	CH ₃ CN cm ⁻¹	THF cm ⁻¹	Pentane cm ⁻¹
Parent bands	2090, 2052, 2024	2089, 2050, 2022	-
‘Hot’ species	2071, 2042, 2005	2079, 2041, 2002	-
Triplet diradical	2080, 2046, 2009	2084, 2046, 2007	-

Table 5 IR data for compound **3**, and the bands observed in the IR spectrum following excitation at 400 nm.

Time resolved IR spectra and kinetics



Compound 1 in Pentane



Compound 2 in THF

6. References

- i Towrie, M.; Grills, D. C.; Dyer, J.; Weinstein, J. A.; Matousek, P.; Barton, R.; Bailey, P. D.; Subramaniam, N.; Kwok, W. M.; Ma, C. S.; Phillips, D.; Parker, A. W.; George, M. W., *Appl. Spectrosc.*, **2003**, *57*, 367-380.
- ii (a) Sonogashira, K.; Tohda, Y.; Hagihara, N., *Tetrahedron Lett.*, **1975**, 4467. (b) Negishi, E.-I.; Anastacia, L., *Chem. Rev.*, **2003**, *103*, 1979.
- iii Park, S.B.; Alper, H., *Chem. Comm.*, **2004**, *11*, 1306.
- iv Champeil, E. ; Draper, S.M., *J. Chem. Soc., Dalton Trans.*, **2001**, 1440-1447
- v Monalti, M.; Credi, A.; Prodi, L.; Gandolfi, M. T. *Handbook of Photochemistry*, 3rd Ed. Taylor and Francis, Boca Raton, **2006**
- vi Platts, J. A.; Evans, G. J. S.; Coogan, M. P.; Overgaard, J. *Inorg. Chem.* **2007**, *46*, 6291-6298
- vii Frisch, M. J. ; Trucks, G. W.; Schlegel, H. B.; Scuseria, G. E.; Robb, M. A.; Cheeseman, J. R.; Montgomery, J. J. A.; Vreven, T.; Kudin, K. N.; Burant, J. C.; Millam, J. M.; Iyengar, S. S.; Tomasi, J.; Barone, V.; Mennucci, B.; Cossi, M.; Scalmani, G.; Rega, N.; Petersson, G. A.; Nakatsuji, H.; Hada, M.; Ehara, M.; Toyota, K.; Fukuda, R.; Hasegawa, J.; Ishida, M.; Nakajima, T.; Honda, Y.; Kitao, O.; Nakai, H.; Klene, M.; Li, X.; Knox, J. E.; Hratchian, H. P.; Cross, J. B. ; Adamo, C.; Jaramillo, J.; Gomperts, R.; Stratmann, R. E.; Yazyev, O.; Austin, A. J.; Cammi, R.; Pomelli, C. J.; Ochterski, W.; Ayala, P. Y.; Morokuma, K.; Voth, G. A.; Salvador, P.; Dannenberg, J. J.; Zakrzewski, V. G.; Dapprich, S.; Daniels, A. D.; Strain, M. C.; Farkas, O.; Malick, D. K.; Rabuck, A. D.; Raghavachari, K.; Foresman, J. B.; Ortiz, J. V.; Cui, Q.; Baboul, A. G.; Clifford, S.; Cioslowski, J.; Stefanov, B. B.; Liu, G.; Liashenko, A.; Piskorz, P.; Komaromi, I.; Martin, R. L.; Fox, D. J.; Keith, T.; Al-Laham, M. A. Peng, C. Y.; Nanayakkara, A.; Challacombe, M.; Gill, P. M. W.; Johnson, B.; Chen, W.; Wong, M. W.; Gonzalez C.; Pople, J. A. Gaussian, Inc., Wallingford CT, **2004**.
- viii Iwashita, Y.; Tamura, F.; Nakamura, A., *Inorg. Chem.* **1969**, *8*, 1179-1183